Supersonic Flutter of Partially Liquid-Filled Circular Cylindrical Shells Subjected to Internal Pressure and Axial Compression

Farhad Sabri[1], Aouni A. Lakis[2]
Applied Mechanics Section, Department of Mechanical Engineering
École Polytechnique de Montréal
C.P. 6079, Succursale Centre-ville, Montréal, Québec, H3C 3A7
CANADA
aouni.lakis@polymtl.ca

Abstract: - This study is focused on the aeroelastic behavior of a circular cylindrical shell in a supersonic airflow. The method of analysis is a combination of Sander's thin shell theory and the classic finite element method. Potential theory is applied to model the effect of the hydrodynamic pressure, and piston theory to derive the aerodynamic damping and stiffness matrices. The influence of stress stiffness due to internal pressure and axial compression is also taken into account. Aeroelastic equations in hybrid finite element formulation are derived and solved numerically. In all study cases the shell loses its stability due to coupled-mode flutter and a traveling wave is observed during this dynamic instability. The results are compared with existing experimental data and other analytical and finite element solutions. The presented study shows efficient and reliable results which can be applied for aeroelastic design and analysis of shells of revolution in aerospace vehicles.

Key-Words: -Aeroelasticity, Flutter, Cylindrical Shell, Hybrid Finite Element, Dynamic, Piston Theory, Potential Flow

1 Introduction

Shells and plates are key elements in the structure of aerospace vehicles. For example, they are used commonly in the fuselage and engine nacelles of airplanes and space shuttles. As they are exposed to an external airflow, particularly supersonic flow, dynamic instability, flutter, becomes key consideration in the design and analysis of skin panels. Circular cylindrical shells can also show this kind of aeroelastic instability and prevention of this behavior is one of the primary design criterions faced by aeronautical engineers. Especially, the fluid-structure interaction in a fuel tank of a liquid propellant rocket has been an important issue during design.

After introducing the application of piston theory in the aeroelastic models presented by Ashley and Zartarian[1], a number of interesting experimental[2] and theoretical[3-7] studies were conducted to investigate supersonic flutter of a cylindrical shell in the late 1960s. In general, all of these works were concerned with the development of an analytical relation to describe the effect of shell and flow parameters on the critical flutter frequency. Aeroelastic models were developed by applying the theory of shells (i.e., linear or nonlinear Donells shallow-shell theory) in conjunction with linear or nonlinear piston theory to account for fluid-structure interaction. The resulting governing equations were treated numerically using the Galerkin method. In most cases the theory did not agree well with experimentally obtained results [8].

There are also some researchers who focused on the numerical solution of this problem. They developed their solutions using a variational formulation. For example, based on the principle of virtual displacements, the variational equations were solved using the finite element method (FEM). Aeroelastic governing equations were derived by applying classical shell theory based on the Kirchchoff-Love hypothesis coupled with the piston theory for evaluation of aerodynamic forces. Bismarck-Nasr[9] developed a FEM applied to the supersonic flutter of a circular shell subjected to internal pressure and axial loading. The numerical results were compared with experimental and analytical solutions. Ganapathi et al [10] modeled an orthotropic and laminated anisotropic circular cylindrical shell in the supersonic flow using FEM and did a parametric study to see the effect of different shell geometries on the flutter boundaries. For more details interested readers can refer to the review paper presented by Bismarck-Nasr[11].

For such a problem that contains complex structures,

[1] PhD Candidate
[2] Professor

boundary conditions, materials, and loading, an analytical model becomes very complicated to undergo for change of all factors affecting the flutter boundaries; therefore, numerical methods like FEM are considered such as powerful tools. The first objective of this study is to adequately describe supersonic flutter of a circular cylindrical shell and present a numerical model of existing experimental data. The second objective is to determine an efficient choice of shell theory for developing a finite element model. Most of the published papers in the literature have applied general linear or nonlinear shell theory based on the Kirchhof-Love hypothesis. These developments can only be applied to thin and uniform shells. In cases of multi-layered shells or shells of non-uniform thickness (i.e. allowing for axial variation in thickness), difficulties occur during the calculation of panel flutter. This work is focused on the development of a circumferential hybrid element for a circular cylindrical shell in the supersonic flow. The procedure is similar to the finite element development done for vertical shells by Lakis and Paidoussis[12] and for horizontal open shells by Selmane and Lakis[13]. These developments resulted in precise and fast convergence with few numerical difficulties. The linear theory developed here is adequate to predict the onset of flutter, however nonlinear shell theory required to capture the actual limit cycle amplitudes of flutter, is left for future study.

2 Structural Modeling

2.1 Hybrid Element

Sander's[14] shell theory is based on Love's first approximation where the inconsistency related to the fact that strains for small rigid-body rotations of the shell do not vanish, has been removed. A circumferential cylindrical frustum based on the development done by Lakis and Paidoussis[12] is applied to generate the mass and stiffness matrices of the structural model. This element type (see Fig. 1) has two nodal circles with two nodal points; i and j. There are four degrees of freedom at each node; axial, radial, circumferential displacement, and rotation. This kind of element makes it possible to use thin shell equations easily in order to find the exact solution of displacement functions rather than an approximation with polynomial functions as is done in classical FEM. This element selection results in a hybrid element where the convergence criterion of the finite element method is provided with greater accuracy.
Considering the displacement in the normal manner, as:

$$\begin{aligned} U(r,x,\theta) &= \sum_n u_n(x)\cos(n\theta) \\ W(r,x,\theta) &= \sum_n w_n(x)\cos(n\theta) \\ V(r,x,\theta) &= \sum_n v_n(x)\sin(n\theta) \end{aligned} \tag{1}$$

where n is the circumferential wave number, and

$$\begin{aligned} u_n(x) &= Ae^{\lambda x/R} \\ v_n(x) &= Be^{\lambda x/R} \\ w_n(x) &= Ce^{\lambda x/R} \end{aligned} \tag{2}$$

Lakis and Paidoussis[12] found the exact analytical solution for displacements as:

$$\begin{Bmatrix} U(x,r,\theta) \\ W(x,r,\theta) \\ V(x,r,\theta) \end{Bmatrix} = [N]\begin{Bmatrix} \delta_i \\ \delta_j \end{Bmatrix} \tag{3}$$

Where

$$\{\delta_i\} = \begin{Bmatrix} u_{ni} \\ w_{ni} \\ (dw_n/dx)_i \\ v_{ni} \end{Bmatrix} \tag{4}$$

$$[N] = [T][R][A]^{-1}$$

Details of this solution can be found in Ref. [12]. The strain vector based this displacement field can be written as:

$$\{\varepsilon\} = [B]\begin{Bmatrix} \delta_i \\ \delta_j \end{Bmatrix} \tag{5}$$

and the stress vector becomes as:

$$\{\sigma\} = [P][B]\begin{Bmatrix} \delta_i \\ \delta_j \end{Bmatrix} \tag{6}$$

Therefore the mass and stiffness matrices for each element are derived as:

$$\begin{aligned} [m] &= \rho h \iint [N]^T[N]dA \\ [k] &= \iint [B]^T[P][B]dA \end{aligned} \tag{7}$$

where ρ is the shell density and $dA = rdxd\theta$. For the entire shell geometry, the standard assembly technique in FEM can be used along with application of the

appropriate boundary conditions to find the global mass and stiffness matrices.

2.2 Initial Stress Stiffness

The influence of membrane forces on the dynamic stability of a cylindrical shell in the presence of supersonic airflow is investigated here. These membrane forces are due to pressure differential across the shell P_m and axial compression P_x . It is assumed that the shell is in an equilibrium condition and also it has not reached its buckling state. The initial in-plane shear, static bending and transverse shear are also ignored for this analysis. The stress resultants due to internal pressure P_m and axial compression P_x are

$$\overline{N}_x = -\frac{P_x}{2\pi R} \qquad \overline{N}_\theta = P_m R \tag{8}$$

The potential energy due to this initial strain is equal to[13]

$$U_i = 1/2 \int_0^l \int_0^{2\pi} [\overline{N}_x \phi_{\theta\theta}^2 + \overline{N}_\theta \phi_{xx}^2 + (\overline{N}_x + \overline{N}_\theta)\phi_n^2] R d\theta dx \tag{9}$$

where l is the element length, ϕ_{xx} is the strain rotation about the x axis, $\phi_{\theta\theta}$ is about the normal to $x\theta$ plane and ϕ_n is the rotation about the normal to the shell element [14].

If the displacements are replaced by Eq. (3), the potential energy in terms of nodal degrees of freedom is generated as:

$$U_i = 1/2 \int_0^l \int_0^{2\pi} \{r\}^T \begin{bmatrix} \overline{N}_x & 0 & 0 \\ 0 & \overline{N}_\theta & 0 \\ 0 & 0 & \overline{N}_x + \overline{N}_\theta \end{bmatrix} \{r\} R d\theta dx \tag{10}$$

where

$$\{r\} = \begin{bmatrix} 0 & -\frac{\partial}{\partial x} & 0 \\ 0 & -\frac{1}{R}\frac{\partial}{\partial \theta} & 0 \\ -\frac{1}{2R}\frac{\partial}{\partial \theta} & 0 & \frac{1}{2}\frac{\partial}{\partial x} \end{bmatrix} \begin{Bmatrix} U \\ W \\ V \end{Bmatrix} = [C_0][N] \begin{Bmatrix} \delta_i \\ \delta_j \end{Bmatrix} \tag{11}$$

and finally the stress stiffness matrix can be written as:

$$[k_I] = \int_0^l \int_0^{2\pi} [N]^T [C_0]^T \begin{bmatrix} \overline{N}_x & 0 & 0 \\ 0 & \overline{N}_\theta & 0 \\ 0 & 0 & \overline{N}_x + \overline{N}_\theta \end{bmatrix} [C_0]^T [N]^T R d\theta dx \tag{12}$$

After assembling the whole initial stiffness matrix, it is added to the global stiffness matrix calculated in Sec. 2.1 for further analysis.

3 Fluid Loading

3.1 Piston Theory

Piston theory is a powerful tool for aerodynamic modeling in aeroelasticity. For a cylinder subjected to an external supersonic airflow parallel to the centerline of the shell, the fluid-structure effect due to external pressure loading can be taken into account using linearized first-order potential theory with (or without) the curvature correction term,[16],[17]:

$$P_a = \frac{\gamma p_\infty M^2}{(M^2-1)^{1/2}} \left[\frac{\partial W}{\partial x} + \frac{M^2-2}{M^2-1} \frac{1}{U_\infty} \frac{\partial W}{\partial t} - \frac{W}{2R(M^2-1)^{1/2}} \right] \tag{13}$$

where p_∞, U_∞, M and γ are the freestream static pressure, freestream velocity, Mach number and adiabatic exponent of air, respectively. If the Mach number is sufficiently high ($M \geq 2$) and neglecting the curvature term $\frac{W}{2R(M^2-1)^{1/2}}$, this equation simplifies to yield the so-called linear piston theory [1]:

$$P_a = -\gamma p_\infty \left[M \frac{\partial W}{\partial x} + \frac{1}{a_\infty} \frac{\partial W}{\partial t} \right] \tag{14}$$

where a_∞ is the freestream speed of sound. Replacing the displacement from Eq. (3), the pressure is found in terms of nodal degree of freedom as (for example, Eq. (14)):

$$\{P_a\} = \begin{Bmatrix} 0 \\ p_{radial} \\ 0 \end{Bmatrix} = -\gamma \frac{p_\infty}{a_\infty} [T][R_f][A^{-1}] \begin{Bmatrix} \dot{\delta}_i \\ \dot{\delta}_j \end{Bmatrix} - (i\frac{\lambda_j}{R}) \gamma p_\infty M [T][R_f][A^{-1}] \begin{Bmatrix} \delta_i \\ \delta_j \end{Bmatrix} \tag{15}$$

3.2 Potential Flow

In cylindrical coordinate system the governing equation for velocity potential ϕ satisfying Laplace equation, is expressed as:

$$\frac{\partial^2 \phi}{\partial r^2} + \frac{1}{r}\frac{\partial \phi}{\partial r} + \frac{1}{r}\frac{\partial^2 \phi}{\partial \theta^2} + \frac{\partial^2 \phi}{\partial x^2} = 0 \tag{16}$$

Using Laplace equations for potential flow accompanied by boundary conditions defined by an impermeability condition and Bernoulli's equation, the linear pressure

loading on the shell wall is given by:

$$P_a = -\rho_f Z\left[\frac{\partial^2 W}{\partial t^2} + 2U_\infty \frac{\partial^2 W}{\partial x \partial t} + U_\infty^2 \frac{\partial^2 W}{\partial x^2}\right] \quad (17)$$

where ρ_f is fluid density. In the above equation, Z which is expressed in terms of Bessel functions of the first and second kind, is found in the Ref. [18]. Upon replacement of displacement from Eq. (3) this pressure loading in terms of nodal degree of freedom becomes:

$$\{P_a\} = \begin{Bmatrix} 0 \\ p_{radial} \\ 0 \end{Bmatrix} = -\rho_\infty Z[T][R_f]\begin{Bmatrix} \ddot{\delta}_i \\ \ddot{\delta}_j \end{Bmatrix} - 2(i\frac{\lambda_j}{R})\rho_\infty U_\infty Z[T][R_f]\begin{Bmatrix} \dot{\delta}_i \\ \dot{\delta}_j \end{Bmatrix} + (\frac{\lambda_j}{R})^2 \rho_\infty U_\infty^2 Z[T][R_f]\begin{Bmatrix} \delta_i \\ \delta_j \end{Bmatrix} \quad (18)$$

3.3 Aerodynamic Damping and Stiffness

The general force vector due to the pressure field is written as:

$$\{F_p\} = \iint [N]^T \{p_a\} dA \quad (19)$$

For example, using the piston theory to account for pressure loading, Eq. (15) can be substituted into Eq. (17) and the aerodynamic damping, $[c_f]$, and stiffness, $[k_f]$, for each element can be found as:

$$[c_f] = [A^{-1}]^T [D_f][A^{-1}]$$
$$[k_f] = [A^{-1}]^T [G_f][A^{-1}] \quad (20)$$

where

$$[D_f] = -\frac{\gamma}{a_\infty} p_\infty \pi r \int_0^l [R]^T [R_f] dx$$
$$[G_f] = -i\frac{\lambda_j}{r} \gamma p_\infty M \pi r \int_0^l [R]^T [R_f] dx \quad (21)$$

In a case of potential flow for pressure loading, upon substitution in Eq. (17), it yields also to fluid mass matrix as:

$$[m_f] = -\rho_f [A^{-1}]^T [S_f][A^{-1}] \quad (22)$$

where

$$[S_f] = \pi r \int_0^l [R]^T [R_f] dx \quad (23)$$

4 Aeroelastic Model in FEM

The governing equation of motion for a fluid filled cylindrical shell subjected to an external supersonic flow under combined internal pressure and axial compression can be written in the following form as:

$$[M_s - M_f]\begin{Bmatrix} \ddot{\delta}_i \\ \ddot{\delta}_j \end{Bmatrix} - [C_f]\begin{Bmatrix} \dot{\delta}_i \\ \dot{\delta}_j \end{Bmatrix} + [\,[K_s] + [K_I] - [K_f]\,]\begin{Bmatrix} \delta_i \\ \delta_j \end{Bmatrix} = 0 \quad (24)$$

where subscripts *s* and *f* refer to a shell in vacuo and fluid, respectively and *I* refers to a shell under axial compression and/or pressurized.

In order to find the aeroelastic behavior of a shell, eigenvalues and eigenvectors of Eq. (22) are found by means of the equation reduction method.

5 Results and Discussion

In this section, numerical results are compared with existing experimental data [2], analytical [3, 6, 7] and numerical [9, 10] solutions. In all of these studies shell geometry and flow parameters have the following similar features:

$$\begin{aligned} &E = 16\times10^6\ lb/in \quad (11\times10^{10}\ N/m^2) \\ &\upsilon = 0.35 \\ &h = 0.0040\ in \quad (0.0001015\ m) \\ &L = 15.4\ in \quad (0.381\ m) \\ &R = 8.00\ in \quad (0.203\ m) \\ &\rho_s = 0.000833\ lb-s^2/in^4 \quad (8900\ kg/m^3) \\ &M = 3.00 \\ &a_\infty = 8400\ in/s \quad (213\ m/s) \\ &T_{t\infty} = 120^\circ F \quad (48.90^\circ C) \end{aligned} \quad (25)$$

where $T_{t\infty}$ is the freestream stagnation temperature and ρ_s is the shell density . This set of data was taken from the experiments done by Olson and Fung[2, 3] in the NASA Ames Research Center (here referred to as case-I). It is necessary to mention that in some of references [6, 9] different values for $L = 16\ in$, $E = 13\times10^6\ lb/in^2$ and $\upsilon = 0.33$ have been used (referred to as case-II). As a consequence, in the present analysis comparison of numerical results was sought for each given set of data.

For both sets of data (case-I and II), numerical results of this study compared to experimental, theoretical and numerical analyses are presented in Table 1. In all of the cases, instability occurred in the form of coupled-mode

flutter. The proposed FEM shows very good agreement with experimental and analytical results and also has better capabilities for aeroelastic stability prediction in terms of critical p_∞ and n compared to the other FEM methods. In Fig. 2 the results of flutter boundary for two different aerodynamic theories; piston and potential theory have been presented and compared with the experimental data of Ref. 3. It can be seen that both theories predict a larger stabilizing effect of the shell internal pressure than the experiments. It also indicates that the potential solution for flutter boundary is higher than that found using piston theory, and the critical value of the circumferential wave number n is somewhat smaller than predicted by piston theory. This is due to the dependency of the pressure field on n in potential theory. As n increases, the pressure decreases significantly. In piston theory the pressure field and n are independent. Therefore, a lower value of n is reached at the flutter boundary. The further analysis in this study is therefore done by applying the piston theory as an aerodynamic model to account for fluid structure interaction in a supersonic flow.

Figure 3 shows some typical complex frequencies versus freestream static pressure, p_∞ for $n = 25$. Only the first and second modes are shown ($m = 1,2$). Aerodynamic pressure is evaluated using piston theory. In Fig. 3a the real part of the complex frequency for the first mode increases while for the second mode it decreases as p_∞ increases. For higher values of p_∞ these real parts eventually merge into a single mode. If p_∞ is increased still further, the shell loses stability at $p_\infty = 0.521\ psi$. This instability is due to coupled-mode flutter because the imaginary part of the complex frequency (which represents the damping of the system) crosses the zero value (see Fig. 3b) and makes the vibration amplitude grow.

In Fig. 4, the flutter boundary for the shell geometry of case-II under different internal pressures P_m is shown. The lowest critical value of freestream static pressure for each circumferential wave number becomes larger when P_m is increased. It is observed that shell internal pressure has a stabilizing influence. Note that experiments[2] demonstrated that for moderate values of P_m the shell loses it dynamic stability up to even unpressurized level while small and high values of P_m stabilize the shell completely (see Fig. 2). This behavior is explained quite well by considering shell imperfections during the analysis[6, 18]. The effect of axial compression on the flutter boundary is also shown in Fig. 4. The axial load P_x decreases the stiffness of the shell which results in a lower critical freestream static pressure than an unstressed shell.

Figure 5 shows the critical value of freestream static pressure for different filling ratio for various length of shell. In general, the critical p_∞ for empty shell increases as the length ratio is decreased. It is seen that for the lower filling ratio, the critical freestream static pressures change rapidly and widely as the filling ratio is increased. By increasing the length ratio the decrement of the critical value of p_∞ is decreases or vanished. This rapid change in the low filling ratio and steady critical p_∞ in the large filling ratio indicates that the fluid near the bottom of shell is influenced more by elastic deformation of shell subjected to the external supersonic flow.

6 Conclusion

An efficient hybrid finite element method is used to analyze the dynamic stability of circular cylindrical shells subjected to external supersonic flow. Linear Sander's shell theory with two different potential and piston theories to account for the aerodynamic pressure field is used in a combined approach to derive the aeroelastic equation of motion. It is observed that piston theory provides a better approximation to account for fluid–structure interaction in supersonic airflow conditions. Numerical results are obtained for different shell boundary conditions and geometries. In all the study cases, only one type of instability is found, namely coupled-mode flutter mostly, in the first and second longitudinal modes. There is a good agreement for prediction of flutter onset with existing experiments and other analytical and FEM analyses. This proposed hybrid FEM provides the capability to apply different theories with different complex boundaries and geometries for an empty or partially liquid-filled circular cylindrical shell. This can be used effectively in the design and analysis of aerospace structures. Reliable results can be obtained at less computational cost compared to commercial FEM software, which imposes some restrictions when such an analysis is done.

References:

[1] Ashley, H. and G. Zartarian, "Piston Theory-New Aerodynamic Tool for Aeroelastician," *Journal of the Aeronautical Sciences*, Vol. 23, NO. 12, 1956, pp. 1109-1118.

[2] Olson, M.D. and Y.C. Fung, "Supersonic Flutter of Circular Cylindrical Shells Subjected to Internal Pressure and Axial Compression," *AIAA Journal*, Vol. 4, NO. 5, 1966, pp. 858-864.

[3] Olson, M.D. and Y.C. Fung, "Comparing Theory and Experiment for Supersonic Flutter of Circular

Cylindrical Shells," *AIAA Journal*, Vol. 5, NO. 10, 1967, pp. 1849-1856.

[4] Evensen, D.A. and M.D. Olson, "Nonlinear Flutter of a Circular Cylindrical Shell in Supersonic Flow," NASA TN D-4265, 1967.

[5] Evensen, D.A. and M.D. Olson, "Circumferentially Traveling Wave Flutter of Circular Cylindrical Shell," *AIAA Journal*, Vol. 6, NO. 8, 1968, pp. 1522-1527.

[6] Carter, L.L. and R.O. Stearman, "Some Aspects of Cylindrical Shell Panel Flutter," *AIAA Journal*, Vol. 6, NO. 1, 1968, pp. 37-43.

[7] Amabili, M. and F. Pellicano, "Nonlinear Supersonic Flutter of Circular Cylindrical Shells," *AIAA Journal*, Vol. 39, NO. 4, 2001, pp. 564-573.

[8] Horn, W., et al., "Recent Contributions to Experiments on Cylindrical Shell Panel Flutter," *AIAA Journal*, Vol. 12, NO. 11, 1974, pp. 1481-1490.

[9] Bismarck-Nasr, M.N., "Finite Element Method Applied to the Supersonic Flutter of Circular Cylindrical Shells," *International Journal for Numerical Methods in Engineering*, Vol. 10, NO. 2, 1976, pp. 423-435.

[10] Ganapathi, M., T.K. Varadan, and J. Jijen, "Field-Consistent Element Applied to Clutter Analysis of Circular Cylindrical Shells," *Journal of Sound and Vibration*, Vol. 171, NO. 4, 1994, pp. 509-527.

[11] Bismarck-Nasr, M.N., "Finite Elements in Aeroelasticity of Plates and Shells," *Applied Mechanics Reviews*, Vol. 49, NO. 10 pt 2, 1996, pp. 17-24.

[12] Lakis, A.A. and M.P. Paidoussis, "Dynamic Analysis of Axially Non-Uniform Thin Cylindrical Shells," *Journal of Mechanical Engineering Science*, Vol. 14, NO. 1, 1972, pp. 49-71.

[13] Selmane, A. and A.A. Lakis, "Non-Linear Dynamic Analysis of Orthotropic Open Cylindrical Shells Subjected to a Flowing Fluid," *Journal of Sound and Vibration*, Vol. 202, NO. 1, 1997, pp. 67-93.

[14] Sanders, J.L., "An Improved First-Approximation Theory for Thin Shell," NASA R-24, 1959.

[15] MacNeal, R.H., "Nastran Theoretical Manual," NASA SP-221, 1972.

[16] Dowell, E.H., *Aeroelasticity of Plates and Shells*, Noordhoff International Publishing, Leyden, 1975.

[17] Krumhaar, H., "The Accuracy of Linear Piston Theory When Applied to Cylindrical Shells," *AIAA Journal*, Vol. 1, NO. 6, 1963, pp. 1448-1449.

[18] Lakis, A.A. and A. Laveau, "Non-Linear Dynamic Analysis of Anisotropic Cylindrical Shells Containing a Flowing Fluid," *International Journal of Solids and Structures*, Vol. 28, NO. 9, 1991, pp. 1079-1094.

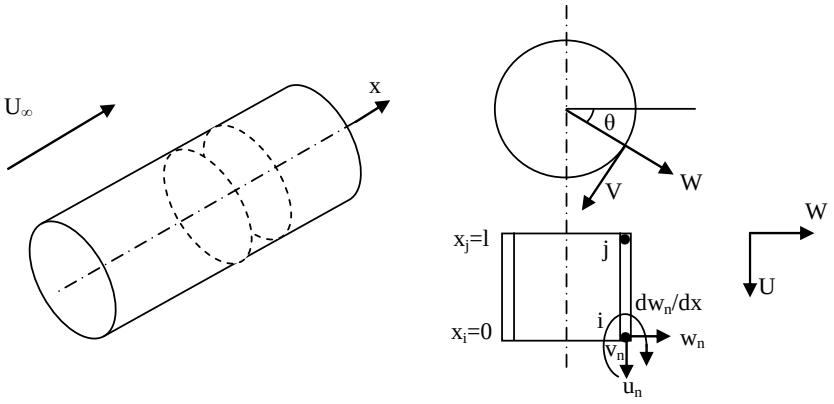

Fig. 1 Geometry of cylindrical frustum element

Table 1 Comparison of shell flutter boundary at $M = 3$ and $p_x = p_m = 0$

	p_∞, psi	$n_{critical}$	L, in	υ	$E, lb/in^2$
Experimental results[2]	0.380-0.420	20	15.40	0.35	16×10^6
Analytical results[6]	0.420	24	16.00	0.33	13×10^6
Analytical results[3]	0.550	25	15.40	0.35	16×10^6
Analytical results[7]	0.330	27	15.40	0.35	16×10^6
FEM results[9]	0.5621	34	16.00	0.33	13×10^6
FEM results[10]	0.5621	25	16.00	0.33	13×10^6
FEM results[10]	0.5621	26	15.40	0.35	16×10^6
Present results	0.522	26	15.40	0.35	16×10^6
Present results	0.382	25	16.00	0.33	13×10^6

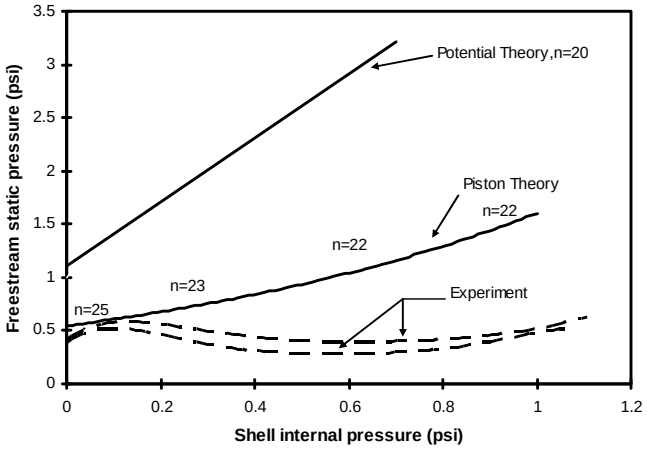

Fig. 2 cylindrical shell flutter boundaries

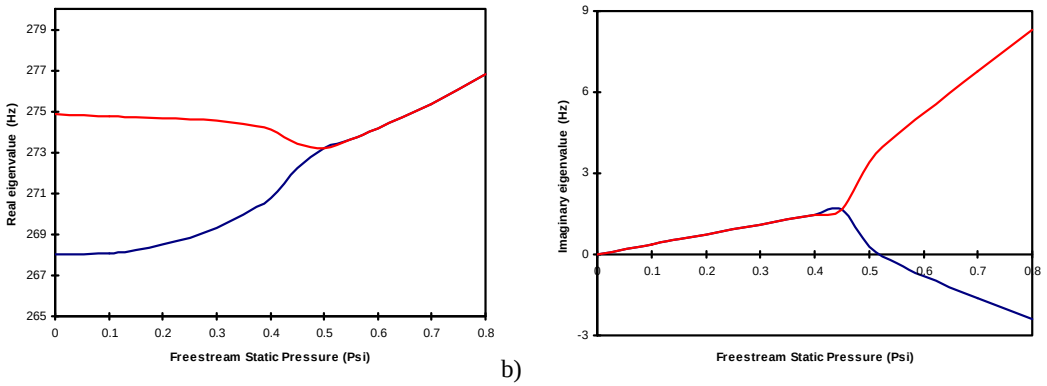

a) b)

Fig. 3 a) Real part and b) imaginary part of the eigenvalues of system vs freestream static pressure, shell case-I, aerodynamic pressure evaluated by piston theory, $n = 25$ $p_m = p_x = 0.0$ psi

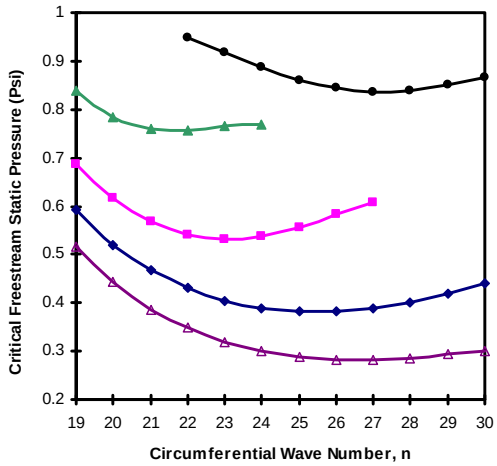

Fig. 4 Flutter boundaries for stressed shell. Shell case-II, $p_x = 0.0$ lb/in^2 : ♦, $p_m = 0.0$ lb/in^2; ■, $p_m = 0.246$ lb/in^2; ▲, $p_m = 0.50$ lb/in^2; ●, $p_m = 0.70$ lb/in^2; Δ, $p_x = 30$ lb, $p_m = 0.0$ lb/in^2.

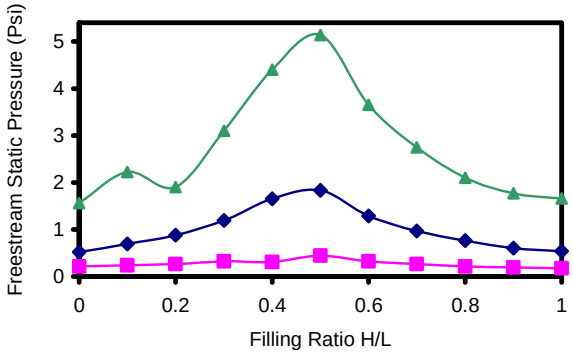

Fig. 5 Flutter boundaries for different H/L: ■, L/R=4; ♦, L/R=2; ▲, L/R=1